A multivariate equivalency and general test for Rensch's Rule: Implications for the evolution of sexual shape dimorphism

Abstract

Rensch's rule, the allometric association between the degree of sexual dimorphism and overall body size, is an important framework for understanding the evolution of trends in phenotypic differentiation between the sexes across taxa. While virtually all recent treatments have explored the degree of sexual size dimorphism, understanding how dimorphism in other phenotypic traits evolves is equally relevant. Indeed, Rensch's original treatment focused not only on size, but also on dimorphism in relative body proportions, coloration, the presence of ornaments, etc. Here, we derive a multivariate equivalency for viewing trends in sexual dimorphism – relative to overall body size – across taxa, and provide a generalized test to determine whether such patterns are consistent with Rensch's rule. For univariate linear traits such as body size, our approach yields equivalent results to those from standard procedures, but our test is also capable of detecting trends in multivariate datasets like shape. Computer simulations reveal the method displays appropriate statistical properties, and an empirical example in Mediterranean lizards illustrates the efficacy of our approach on both univariate and multivariate phenotypes. Our generalized procedure substantially extends the toolkit available for investigating macroevolutionary patterns of sexual dimorphism and seeking a better understanding of the processes that underlie them.

Introduction

It is widely observed that males and females of the same species are not identical, but rather differ – sometimes substantially – in their phenotypic characteristics (Fairbairn 1997, 2013). Indeed, sexual dimorphism is pervasive across many animal clades, and understanding the causes for these patterns has attracted considerable attention in evolutionary biology for well over a century (e.g., Darwin 1871; Fairbairn et al. 2007). One of the most conspicuous differences between males and females is in their body sizes (Andersson 1994), where sex-specific differences are often hypothesized to be the result of selection pressures related to reproduction, or the distinct ecological roles of males and females in their respective habitat (Cox et al. 2003; Stephens and Wiens 2009; Kaliontzopoulou et al. 2015; Tarr et al. 2018; Littleford-Colquhoun et al. 2019). For example, both sexual selection on male body size (Cox et al. 2003; Garcia-Navas et al. 2015; Horne et al. 2020), and fecundity selection on female body size (Serrano-Meneses and Szekely 2006; Stuart-Fox 2008), are expected to enhance the degree of sexual size dimorphism in taxa over evolutionary time. Likewise, when males and females respond differently to environmental factors, intraspecific competition may generate ecological divergence between them, resulting in varying patterns of sexual dimorphism (Butler et al. 2000; Bolnick and Doebeli 2003; Dayan and Simberloff 2005; Kaliontzopoulou et al. 2010; Meiri et al. 2014).

At macroevolutionary scales, changes in the relative contribution of the selective forces above may create variation in the degree of sexual dimorphism displayed across closely related taxa. For instance, sister species inhabiting different environments, or possessing distinct ecological adaptations, may exhibit differing degrees of sexual dimorphism, as a result of the varying intensity of sexual selection they endure (Östman and Stuart-Fox 2011). Likewise, the interplay between sexual and natural selection that species experience may result in sexual dimorphism of differing magnitudes across taxa (Blanckenhorn et al. 2006; Stuart-Fox and Moussalli 2007; Kaliontzopoulou et al. 2015). One evolutionary framework that connects adaptive explanations for the evolution of sexual size dimorphism (SSD) with trends in overall body size across taxa is Rensch's rule. Here it is predicted that SSD will increase with species' average body size in species where males are the larger sex (hyperallometry), and likewise will decrease with increasing body size where females are the larger sex (hypoallometry) (Abouheif and Fairbairn 1997; Fairbairn 1997). Put another way, Rensch's rule predicts that the extent of sexual dimorphism increases at more extreme body sizes (both large and small) across taxa. Empirical studies have documented trends in SSD consistent with Rensch's rule in a wide variety of animal taxa (Dale et al. 2007; Ceballos et al. 2013; Regis and Meik 2017; Johnson et al. 2017). However, other clades display the converse trend (Burbrink and Futterman 2019; Peñalver-Alcázar et al. 2019), and some clades display no relationship between SSD and body size (Astúa 2010; Hirst and Kiørboe

2014; Johnson et al. 2017). From an evolutionary perspective, the association between SSD and body size has been hypothesized to be driven by variation in ontogenetic or static allometries across taxa, which results from the influence of sexual selection on growth and maturation patterns (Rensch 1960; Dale et al. 2007).

Interestingly, virtually all evaluations of Rensch's rule have investigated patterns of sexual size dimorphism, yet Rensch's original contributions were concerned with a much wider array of phenotypic traits that can differ between the sexes. These included not only sexual differences in body size, but also in general body proportions (e.g., relative wing and limb lengths), the degree of complexity of different body structures, the presence of sex-specific ornamentation (e.g., horns, body coloration, etc.), and other sex-specific differences (Rensch 1950, 1960). In like manner, some studies have documented patterns of sexual shape dimorphism (e.g., Berns and Adams 2013; Kelly et al. 2013; Kaliontzopoulou et al. 2015), sex-specific differences in ornamentation (Geist and Bayer 1988; Emlen 2008; Watson and Simmons 2010), or coloration (e.g., Endler 1983). However, such studies have typically been restricted to one or a few taxa, and have not explained macroevolutionary variation in sexual dimorphism in a manner that relates directly to Rensch's rule. Thus, when viewed from this perspective, Rensch's (1950) vision was far more synthetic, as he sought to explain the extent to which sexual dimorphism – across a general suite of phenotypic characteristics – scaled with overall body size in organisms, and why some species displayed a greater degree of sexual dimorphism than did others. Remarkably, patterns of intraspecific static allometry in sexually selected traits establishes a direct link between variation in those traits relative to size, and the evolutionary allometry across taxa in the degree of sexual dimorphism that may be expected (see also Rensch 1960; Reiss 1986; Bonduriansky 2007). Under this framework, the "exaggeration" of body structures or other phenotypic traits with increasing body size is predicted to translate, at macroevolutionary scales, into increased degrees of sexual dimorphism with increasing body size. However, despite this clear prediction, and Rensch's original observations, the evolutionary scaling of the degree of sexual dimorphism in phenotypic traits other than size, remains largely unexplored.

Another current limitation in our understanding of Rensch's rule is the fact that to date, all studies have been conducted exclusively on univariate data, primarily regarding body size. However, understanding phenotypic evolution is inherently a multivariate endeavor (Blows 2007; Collyer et al. 2015; Adams and Collyer 2018, 2019), as processes such as natural and sexual selection simultaneously operate on more than one trait (Lande 1979; Lande and Arnold 1983), and can affect variation in complex multidimensional traits such as shape. To interrogate such patterns, the analytics used to evaluate evolutionary trends in phenotypic datasets must be sufficiently general to accommodate this empirical fact. Unfortunately, all current analytical

3

approaches for evaluating trends in sexual dimorphism as they relate to overall body size are explicitly univariate; thereby excluding the possibility of evaluating patterns in complex multidimensional traits such as organismal shape. Though is has been extensively documented in sexual size dimorphism, it remains unknown whether Rensch's rule applies equally to sexual shape dimorphism, as determining this requires an analytical framework capable of evaluating trends in sexual dimorphism in both univariate and multivariate datasets.

In this paper, we derive a multivariate equivalency for inspecting variation in sexual dimorphism – relative to overall body size – across taxa, and provide a generalized test to determine whether they are consistent with Rensch's rule. Our procedure is appropriate for evaluating trends in univariate traits measured on a linear scale (such as body size or relative limb length), as well as in multivariate datasets representing complex phenotypes (such as sets of body proportions or landmark-based shape data). For univariate data, the approach yields equivalent results to what is normally accomplished for size-based SSD evaluations. However, the approach extends these procedures for the examination of sexual dimorphism in multivariate data, thereby increasing the potential for our conceptual understanding of the consequences of sexual and natural selection on complex organismal phenotypes. We conduct a series of computer simulations demonstrating that the approach displays appropriate statistical properties when evaluating trends in both univariate and multivariate data. We also provide an empirical example in Mediterranean green lizards which illustrates the efficacy of our approach on both univariate and multivariate datasets. Finally, we highlight the new avenues of evolutionary research that our generalization facilitates, and make comments on the prospects for future empirical advances.

Methods and Results

Conceptual Development

To arrive at a general test for Rensch's rule that can accommodate multivariate data, we must first derive a series of mathematical equivalencies based upon how interspecific patterns of size dimorphism are typically evaluated. For sexual size dimorphism, interspecific patterns are often inspected using a bivariate plot, where the size of one sex is plotted against the size of the other sex (e.g., Fairbairn and Preziosi 1994; Abouheif and Fairbairn 1997; Ceballos et al. 2013). An idealized example is shown in Fig. 1A, with male size plotted against female size. The diagonal line represents no size dimorphism; or a 1:1 size ratio between the sexes across the range of body sizes for species in the clade of interest. In this construction (i.e., with females plotted on the x-axis), deviations from this line represent differential trends in size

4

dimorphism across taxa. To evaluate such patterns statistically, a phylogenetic regression is performed, and in this case, a slope significantly greater than 1.0 (i.e., $\beta_1 > 1.0$) would be treated as evidence that the evolutionary changes in sexual size dimorphism across taxa are consistent with Rensch's rule (Fairbairn 1997).

An equivalent representation of patterns of sexual dimorphism may also be found using ratios (e.g., male size:female size). When plotted against the average size for each species (Fig. 1B), the same information is conveyed as is found in the more commonly utilized male - female plot of Fig. 1A. However, in this representation, the line designating no sexual dimorphism is horizontal, with a slope of zero (i.e., $\beta_1 = 0.0$) and an intercept of 1.0. As before, a phylogenetic regression may be performed on these data, and in this case, if the slope is significantly steeper than zero (i.e., $\beta_1 > 0.0$), patterns consistent with Rensch's rule are observed.

A third equivalency is shown in Fig. 1C. Here, the Euclidean distance between male and female means for each species ($D_{SD} = \sqrt{(Y_{male} - Y_{female})^2}$) is shown relative to the overall size of the species. This plot is similar to a Bland-Altmann plot (Altman and Bland 1983), except that the Euclidean distance, rather than a difference score, is plotted along the y-axis (as distances can accommodate data of different dimensionality). Under Rensch's rule, this *sexual dimorphism distance* may become greater as species are progressively larger (hyperallometry, sensu Abouheif and Fairbairn 1997) or may become greater as species are progressively smaller (hypoallometry, sensu Abouheif and Fairbairn 1997). In both cases, patterns correspond to species displaying progressively more sexual dimorphism at extreme body sizes; a trend consistent with Rensch's rule. Note that the inflection point in Fig. 1C represents an intermediate size where there is no sexual dimorphism for the trait, and corresponds to where the male-female regression line of Fig. 1A crosses the line representing no sexual dimorphism. This inflection point may represent the overall mean size across species in the lineage, or may be some other value. For instance, in some lineages (e.g., turtles: Ceballos et al. 2013), nearly all species are female biased, in which case the inflection point for D_{SD} vs. size would be found at the far-right end of the plot.

Finally, from D_{SD} a *sexual dimorphism distance index* ($SDDI$) may be constructed as:

$$SDDI = -1 * D_{SD}$$

$$SDDI = +1 * D_{SD}$$

Here, D_{SD} is multiplied by either a +1 or -1, based on a comparison of male and female trait values for

the species. For instance, when single-valued traits on a linear scale are examined (e.g., leg length or wing extent), D_{SD} is multiplied by -1 for those species where females display larger values than males, and remains unchanged for species where males are larger than females. This logic is analogous to that of Lovich and Gibbons (1992) for their index of overall body size dimorphism. However, from a geometric perspective, this procedure is tantamount to determining which species in Fig. 1A are found below the 1:1 size line (i.e., the line representing no size dimorphism), and multiplying those species' D_{SD} by -1.

Unfortunately, applying the same logic to multidimensional trait data is more complicated, as sex-specific differences are not always guaranteed to align with some *a priori* direction in the multivariate dataspace. Thus, for multivariate datasets, one of two procedures may be used. First, for multivariate sets of traits that are measured on the same linear scale (e.g., length, width, and height measures), one could envision a hyperdimensional version of the plot displayed in Fig. 1A, but where the set of male traits are plotted against the set of female traits. In this construction, because the traits are quantified on the same measured scale, the 1:1 size vector representing no sexual dimorphism does exist, and emanates from the origin of the space extending in a positive direction as the trait values increase. To determine whether male trait values deviate more from this vector than do female trait values, a partial least squares analysis may be performed (Rohlf and Corti 2000). Partial least squares (PLS) is a multivariate association procedure which describes the covariation between sets of traits (in this case, between the set of male traits and the set of female traits). Scores along the first PLS axis represent the maximal covariation between male and female traits projected to a single dimension, and species whose male and female PLS scores are identical are those displaying no sexual dimorphism. Thus, deviations from that pattern represent instances of multivariate sexual dimorphism. By plotting these scores, one may determine which species display female scores (on PLS_1) that are larger than their corresponding male scores (when negative values on PLS_1 correspond to smaller individuals; otherwise, the converse comparison is used). The D_{SD} for these species may then be multiplied by -1 to obtain the $SDDI$ for that species. Note that when PLS is used on univariate data, this procedure obtains values identical to those from the method described previously where male and female sizes are compared directly. Thus, for multivariate traits measured on a linear scale, this is a direct generalization of the standard univariate procedure (see empirical example below).

Alternatively, one might be interested in examining multidimensional traits other than linear biometric measurements, such as color or shape. For instance, one may characterize the shape of males and females using geometric morphometric methods (Bookstein 1991; Mitteroecker and Gunz 2009; Adams et al. 2013),

where the locations of anatomical landmarks and semilandmarks are used to obtain a set of shape variables. Geometric morphometric methods also result in a multidimensional characterization of phenotypic traits, from which the degree of sexual dimorphism for each species may be quantified using D_{SD}. However, because the resulting shape variables do not have a one to one correspondence with linear size measures, there is no *a priori* direction in the multivariate shape space that is equivalent to the 1:1 size vector found with sets of linear traits. In fact, for the case of isometry (i.e., shape does not change as size changes), all observations are represented by a single location in the shape space. Thus, while a PLS of male shapes versus female shapes will describe the covariation between them, this direction is not guaranteed to align with size, because there is no direction in the shape space that may be used to unambiguously determine whether dimorphism is male- or female-biased, as for shape variables there is no *a priori* directionality. Nonetheless, one may still quantitatively determine whether the degree of sexual shape dimorphism covaries with overall body size, by using the sexual dimorphism index as defined by the dimorphism distance (i.e., $SDDI = D_{SD}$) to represent the degree of multivariate shape dimorphism for each species.

Once the sexual dimorphism distance index ($SDDI$) is calculated, it may be evaluated against the average size of each species. Here, data conforming to Rensch's rule will result in significant trends of sexual dimorphism relative to mean body size (Fig. 1D). As with size ratios, the line of no sexual dimorphism is a horizontal line, but this time it is centered on zero, as a distance of zero corresponds to no sexual dimorphism. Thus, a phylogenetic regression of these data whose slope is significantly different from zero (e.g., $\beta_1 \neq 0.0$) provides evidence that the evolution of sexual dimorphism is consistent with patterns expected under Rensch's rule. For cases where traits are measured on a linear scale, patterns expected under Rensch's rule exhibit a slope significantly greater than zero ($\beta_1 > 0.0$), as in the usual formulation. Likewise, when using geometric morphometric shape data (or any other type of mean-centered multidimensional data), hyperallometric patterns consistent with Rensch's rule would also display a slope significantly greater than zero ($\beta_1 > 0.0$), indicating that the degree of sexual shape dimorphism increases with increasing body size. Conversely however, hypoallometric patterns would display the opposite pattern ($\beta_1 < 0.0$), indicating that smaller species display greater sexual shape dimorphism.

Simulations

To ascertain the statistical performance of the approach proposed here, we conducted a series of computer simulations. We evaluated the ability of SDDI to characterize patterns of sexual dimorphism in both univariate

7

and multivariate datasets. For each simulation, we generated a pure-birth phylogeny containing 50 species, on which we simulated datasets under a Brownian motion model of evolution. For univariate data ($p = 1$), a single trait was evolved along the phylogeny, and represented the female trait values (x). Next, male values (y) were simulated in such a manner as to generate a known male:female relationship (plus random error), using the function: $y = \alpha x + \mathcal{N}(\mu = 0, \sigma = 0.1)$. For type I error simulations, no sexual dimorphism was generated, meaning that the slope, α, characterized a 1:1 relationship between male and female trait values (i.e., $\alpha = 1.0$). For power simulations, we simulated male values with a slope greater than 1.0 to correspond with patterns following Rensch's rule (i.e., $\alpha = 1.1$). A total of 1,000 datasets were generated under each simulation condition. We then evaluated all datasets using standard approaches (i.e., a phylogenetic regression of male values versus female values), as well as a phylogenetic regression of SDDI versus average body size. The proportion of significant datasets was treated as the type I error ($\alpha = 1.0$) or power ($\alpha = 1.1$) respectively.

For multivariate data ($p = 5$), a slightly different procedure was utilized. First, average body size (s) was evolved along the phylogeny under Brownian motion. Next, female traits ($\mathbf{X}$) were simulated on the phylogeny under Brownian motion, using a $p \times p$ trait covariance matrix with correlations between traits of ($r = 0.7$). For simulations where there was no pattern of sexual dimorphism across species (i.e., type I error simulations) male trait values were then generated by incorporating random error to the female trait values, in a manner analogous to that achieved in the univariate simulations: $\mathbf{Y} = \mathbf{X}_F + \mathcal{N}(\mu = 0, \sigma = 0.1)$. For simulations where patterns of sexual dimorphism covaried with body size (i.e., power simulations), male trait values were generated by incorporating random error to the female trait values, but with the addition that female trait values were pre-multiplied by a scalar value of body size: $\mathbf{Y} = (0.1 * s) * \mathbf{X}_F + \mathcal{N}(\mu = 0, \sigma = 0.1)$. This ensured that male and female trait values covaried with one another as expected, and also covaried with size in the desired direction. As before, a total of 1,000 datasets were generated under each simulation condition. We then evaluated all datasets using a phylogenetic regression of SDDI versus average body size. The proportion of significant datasets was treated as the type I error ($\alpha = 1.0$) or power ($\alpha = 1.1$) respectively.

Simulation Results: For the univariate dataset, we found that both a phylogenetic regression of male size on female size, as well as a phylogenetic regression of $SDDI$ on body size, resulted in appropriate type I error rates near the nominal $\alpha \approx 0.05$ (Fig. 2). Further, when data were simulated under conditions consistent with Rensch's rule, both procedures were capable of detecting the signal of the pattern, and did so with very high power. Thus, using the $SDDI$ approach proposed here was equivalent to what is normally utilized for univariate datasets. Likewise, for multivariate data, the $SDDI$ approach displayed appropriate type I error

8

241 ($\alpha \approx 0.05$) and high statistical power under the conditions simulated (Fig. 2). Additionally, multiplying D_{SD}

242 by ± 1 had little effect on the outcome for multivariate data, as in both cases type I error and power results

243 were virtually identical. Thus, methods for evaluating sexual dimorphism using geometric morphometric

244 data are anticipated to remain robust. Overall results from these simulations imply that using the sexual

245 dimorphism distance index ($SDDI$) proposed here provides an appropriate means of characterizing patterns

246 of sexual dimorphism in both univariate and multivariate traits, and that the procedure is capable of

247 detecting patterns consistent with Rensch's rule when they are present in phenotypic datasets.

248

Empirical Example

250 To illustrate the utility of the approach presented here, we conducted an analysis of both size and shape

251 dimorphism in a group of Mediterranean lizards with extensive body size variation. Our dataset consisted of

252 three data types: male and female values of body size (snout-vent length: SVL), male and female values for

253 a series of head measurements (head length, head width, head height, pileus length, and mouth opening:

254 Fig. 3A), and male and female values of head shape (Fig. 3B). A total of 374 specimens from 21 lineages

255 of green lizards, a monophyletic clade that includes two genera (*Lacerta* and *Timon*), were obtained from

256 natural history museum collections. For each lineage, we obtained samples distributed across the entire

257 distribution range, resulting in an initial database of 1062 specimens. In order to take sampling bias into

258 account, we selected the 10 largest individuals per sex, when sufficient specimens were available, for use in

259 subsequent size and shape analyses. A detailed account of the specimens used for this study is available in

260 the Supplemental Material.

261

262 From these specimens, we calculated mean body size for each sex and lineage. Likewise, we calculated the

263 mean trait values for each sex and lineage for the set of linear measures. These values were then standardized

264 by SVL; resulting in a set of head measurements proportional to body size for each sex $\times$ lineage combination.

265 Additionally, we quantified lateral head shape variation using geometric morphometric methods (Adams et al.

266 2013). This was accomplished by first digitizing 17 landmarks and semilandmarks from images of the right

267 side of the head (Fig. 3B). The thin-plate spline was used to estimate the position of missing landmarks

268 (Gunz et al. 2009), and the position of the jaw relative to the skull was standardized using the fixed angle

269 method (Adams 1999). Next, a generalized Procrustes analysis (Rohlf and Slice 1990) was performed to

270 eliminate non-shape variation from the landmark data and align the specimens to a common coordinate

271 system. The position of semilandmarks (i.e. 11-16, Fig. 3B) was optimized by minimizing the bending energy

²⁷² (Bookstein 1997). From the aligned Procrustes coordinates the mean head shape for males and for females

²⁷³ was then calculated for each lineage. Finally, the phylogenetic relationships among lineages were estimated

²⁷⁴ using published sequences on five mitochondrial and four nuclear gene fragments, totaling 8383 bp. These

²⁷⁵ were then used following standard phylogenetic inference procedures to generate a dated consensus phylogeny

²⁷⁶ for the lineages of interest (for details see Supplemental Material).

²⁷⁷

²⁷⁸ Using these data, we conducted a series of analyses to investigate whether patterns of sexual size dimorphism

²⁷⁹ (SSD) and sexual shape dimorphism (SShD) in this group corresponded to expectations under Rensch's

²⁸⁰ rule. First, we examined patterns of SSD using a phylogenetic regression of male size against female size.

²⁸¹ Here, a slope significantly greater than 1.0 ($\beta > 1.0$) was treated as evidence consistent with Rensch's rule.

²⁸² Additionally, we evaluated SSD patterns using the approach developed here, via a phylogenetic regression of

²⁸³ the sexual size dimorphism index against mean body size for each species. Second, we evaluated multivariate

²⁸⁴ patterns of sexual dimorphism in head proportions in relation to body size, using the sexual dimorphism

²⁸⁵ index obtained from the Euclidean distance between male and female means from each species (D_{SD}).

²⁸⁶ Partial least squares was used to determine which species displayed female scores (on PLS_1) larger than

²⁸⁷ their corresponding male scores, and the sexual dimorphism index was then obtained by multiplying the

²⁸⁸ sexual dimorphism distance by +1 or -1, respectively (i.e., $SDDI = \pm 1 * D_{SD}$). We then performed a

²⁸⁹ phylogenetic regression of $SDDI$ for head proportions versus mean body size to determine whether patterns

²⁹⁰ of dimorphism corresponded to what is expected under Rensch's rule. Third, we obtained the degree of sexual

²⁹¹ dimorphism in head shape for each species using the Procrustes distance between male and female means, and

²⁹² from this calculated the sexual shape dimorphism index ($SShDI$) in their original units as described above

²⁹³ (i.e., $SShDI = D_{SD}$). We then performed a phylogenetic regression of sexual shape dimorphism ($SShDI$)

²⁹⁴ against the mean body size for each species to determine whether patterns of head shape dimorphism were

²⁹⁵ consistent with predictions from Rensch's rule. Additionally, patterns of head shape dimorphism were further

²⁹⁶ investigated using principal components analysis of the set of mean male and female head shapes across

²⁹⁷ species. Finally, we used phylogenetic correlation (phylogenetic partial least squares: sensu Adams and

²⁹⁸ Felice 2014) to determine whether the degree of head shape dimorphism was associated with levels of size

²⁹⁹ dimorphism. All analyses were performed in R 3.6.2 (R Core Team 2019) using the packages `geomorph`

³⁰⁰ (Adams and Otárola-Castillo 2013; Adams et al. 2019), `RRPP` (Collyer and Adams 2018), and routines written

³⁰¹ by the authors.

³⁰²

³⁰³ *Empirical Results*: Using phylogenetic regression, we found a significant relationship between male size and

10

female size, with a slope significantly greater than one ($\beta = 1.39$, $T = 2.91$, $P = 0.009$: Fig. 3C). This indicated that the degree of sexual size dimorphism differed systematically with overall body size; a pattern consistent with that expected under Rensch's rule. In this case, both hypoallometry and hyperallometry (*sensu* Abouheif and Fairbairn 1997) were displayed (Fig. 3C). Specifically, in male-biased species, the degree of sexual dimorphism was greater with increasing body size, and in female-biased species the degree of sexual dimorphism increased in smaller species (though the pattern was more pronounced in male-biased species). Similarly, when using the sexual size dimorphism index (SSDI), we found a significant and positive evolutionary relationship between SSDI and mean body size, confirming the Rensch's rule pattern identified using the commonly-used procedure ($\beta = 0.43$, $F = 22.95$, $Z = 1.89$, $P = 0.004$: Fig. 3D).

When multivariate patterns of sexual dimorphism were evaluated, we found that the degree of dimorphism in head proportions increased as body size increased: a pattern consistent with Rensch's rule ($F = 7.20$, $Z = 1.41$, $P = 0.022$: Fig. 3E). Likewise, when patterns of head shape dimorphism were examined, we found that the degree of sexual shape dimorphism (SShDI) increased in larger species, and a phylogenetic regression of sexual shape dimorphism versus mean body size was found to be significant ($F = 6.05$, $Z = 1.35$, $P = 0.03$: Fig. 3F). Thus, for both multivariate datasets, the degree of sexual dimorphism was enhanced in larger species (hyperallometry; sensu Abouheif and Fairbairn 1997): a pattern consistent with what was expected under Rensch's rule. To our knowledge, this is the first empirical demonstration of a pattern following Rensch's rule in multivariate data.

Visualizing patterns of head shape dimorphism using principal components analysis (Fig. 4), it was evident that males and females occupied distinct regions of morphospace. Further, the head shapes of males and females of the smallest lineage, *Lacerta agilis bosnica*, were distinct from those of the largest species, *Timon lepidus*. When connected, the sexual shape dimorphism vectors for these two species did not coincide with one another in the ordination, implying a difference in sexual shape dimorphism across species. Specifically, the vector for *T. lepidus* was longer than that for *L. agilis bosnica*, which reflected the greater degree of sexual shape dimorphism exhibited by this species. Thin-plate spline deformation grids facilitated a graphical description of these shape differences, where sexual shape dimorphism in *L. agilis bosnica* was best described as a contrast between longer-headed males, with an amplified tympanic area; and short-headed females, with a relatively more reduced tympanic region (Fig. 4, left). By contrast, sexual shape dimorphism in *T. lepidus* was both more prominent in the tympanic area, similarly to what was observed in *L. agilis bosnica*; and also included a modification of the relative lower jaw area. Indeed, males of *T. lepidus* were characterized by both a

11

longer posterior head region and by deeper lower jaw configurations as compared to females of the same species.

Finally, across taxa, the degree of body size and head shape dimorphism were significantly correlated with one another ($r = 0.73$, $p = 0.0001$), but not when evaluated in a phylogenetic context ($r_{PPLS} = 0.361$, $Z = 1.28$, $P = 0.12$). Part of this difference may be explained by the fact that the largest species (i.e. members of the genus *Timon*) - which displayed the greatest degree of both size and shape dimorphism - form a clade within the broader phylogeny for the group (Fig. 5). Thus, despite the strong association of size and shape dimorphism, there were fewer changes of these patterns across branches of the phylogeny. Generally speaking, the degree of size dimorphism and the degree of shape dimorphism increased in larger taxa, and heat maps of the evolution of size and shape dimorphism across the phylogeny indicated a strong association between the two; particularly in large taxa (Fig. 5). Thus, in this system, it appeared that evolutionary changes in size between the sexes were accompanied by concomitant changes in head shape.

Discussion

A longstanding question in evolutionary biology is understanding why sexual dimorphism, the degree of differentiation between the sexes, varies across species. A frequently used schema for exploring macroevolutionary patterns of sexual dimorphism is Rensch's rule, which predicts that sexual dimorphism should increase with body size in species where males are the larger sex, and decrease with increasing body size in species where females are the larger sex. Remarkably, virtually all recent studies have focused on macroevolutionary variation in sexual *size* dimorphism, despite the relevance of sexual dimorphism in other traits, as encompassed by Rensch's original treatment (Rensch 1950). This gap has been driven, in part, by the lack of adequate tools for evaluating Rensch's rule in multivariate traits, such as color, ornament complexity, or shape. In this article, we fill this procedural gap by providing an analytical equivalency that allows the generalization of statistical tests of Rensch's rule for both univariate and multivariate traits. The approach describes the degree of sexual dimorphism as a distance between male and female trait values in phenotype space, thereby facilitating its use on either single-valued traits (e.g., body size), or complex, multivariate traits (e.g. organismal shape). Computer simulations confirm that the approach exhibits appropriate type I error rates and statistical power, thereby providing an adequate procedure for testing whether empirical data comply with the predictions of Rensch's rule. The implementation of our approach on an empirical study of Mediterranean lizards revealed that patterns of sexual dimorphism comply with Rensch's rule not only for body size, but also for relative head proportions and head shape, offering new insights and triggering novel hypotheses about the possible proximate and evolutionary causes that may underlie such patterns.

12

Our empirical example in Mediterranean green lizards exemplifies a case study investigating variation in sexual dimorphism – not only in size – but also in multivariate phenotypes, like shape, and how this method can provide useful insights into the proximate and evolutionary causes underlying such patterns. First, we found that the degree of sexual size dimorphism increased as taxa became larger (Fig. 3C, D). This pattern is compliant with Rensch's rule and corresponds with hyperallometry (Abouheif and Fairbairn 1997), which is to be expected when males are the larger sex (Fairbairn 1997). In this group males are larger than females in most lineages (Fig. 3C), as is commonly observed in lacertids (Braña 1996). Additionally, as in many lizard species, sexual selection in this group is primarily mediated through territoriality, where male-male competition selects for a larger male body size (Stamps 1983). Thus, in this system there is an association between male-biased sexual size dimorphism and male-male competition. As such, the patterns of size dimorphism observed in this study are consistent with those expected under a scenario where sexual selection drives the evolution of larger male body size across taxa via male-male competition.

Likewise, our multivariate analyses revealed that head morphology differed between the sexes, and that the degree of sexual dimorphism in multivariate head shape also corresponded to that expected under Rensch's rule (Fig. 3E, 3F). That is, while both small (e.g. *L. a. bosnica*, Fig. 4, left) and large (e.g. *T. lepidus*, Fig. 4, right) species are sexually dimorphic in head shape, the degree of sexual shape dimorphism increased with average body size (Fig. 3F); a pattern consistent with a scenario of hyperallometry. Examination of the resulting shape differences revealed that sexual dimorphism in head shape was associated with an amplification of the posterior head region, and also in the relative size of the lower jaw (in the case of *T. lepidus*). Biomechanically, these are precisely the anatomical regions where the jaw adductor muscles reside (Haas 1973), and as such, an amplification of these areas in males would enhance biting performance (Herrel et al. 1996; Kaliontzopoulou et al. 2012); a functional trait that has important implications for male competitive capacity (Huyghe et al. 2005; Lailvaux and Irschick 2007). In addition, one might predict that the need for stronger jaw musculature in males becomes disproportionately more intense with increasing body size, as male combats are expected to be more fierce among larger-bodied opponents. Thus, our findings that head shape dimorphism increases with overall body size is also consistent with the hypothesis that sexual selection on structures related to territoriality and male competitive interactions are responsible for the macroevolutionary patterns of sexual shape dimorphism observed in this group. To our knowledge, this is the first example of Rensch's rule in a multivariate phenotype.

13

With respect to the analytical approach proposed here, our characterization of sexual dimorphism via a *shape distance* and the $SDDI$ statistic is completely general, and may be used to evaluate evolutionary trends in any continuous, quantitative trait that differs between the sexes. Our empirical example highlighted the efficacy of the approach for evaluating trends in univariate traits such as body size, and also several types of complex data where organismal phenotypes are quantified by multiple dimensions. As such, the approach developed here expands our current analytical toolkit to provide a means of evaluating evolutionary trends in sexual dimorphism for a broader class of phenotypic traits than has previously been considered. Indeed, this advance more closely embodies Rensch's (1950) original conceptualization for understanding patterns of sexual dimorphism, as his broader vision was to explain why phenotypic differences *writ large* exist among the sexes. Thus, use of the $SDDI$ will facilitate a greater degree of evolutionary exploration into patterns of sexual dimorphism than has been possible in recent decades. Further, with the inclusion of multivariate traits, the formulation proposed here opens the door for investigations into the evolution of sexual shape dimorphism, and whether such patterns correspond to those expected under Rensch's rule. Thus, the mathematical test proposed here is general, and may be used for any quantitative phenotypic trait under scrutiny.

Finally, because $SDDI$ is derived from a phenotypic distance, one could, in theory, utilize the approach to characterize patterns of sexual dimorphism in non-continuous traits, and determine quantitatively whether the degree of sexual dimorphism is enhanced with increasing body size. Across the tree of life, major phenotypic adaptations are often described as evolutionary innovations or novelties (sensu Wagner and Altenberg 1996; Wagner and Muller 2002; Peterson and Müller 2016), where these changes are characterized as discrete shifts from one phenotypic state to another (O'Keefe et al. 2011; e.g., Holliday and Gardner 2012). In like manner, discrete phenotypic differences are known to exist between the sexes; for instance where males display horns or other ornamentation (Geist and Bayer 1988; Emlen 2008) that females lack. Over evolutionary time, a series of such discrete phenotypic differences may accumulate in males relative to females, resulting in an elaboration of phenotypic differences between the sexes in suites of such traits. With an appropriate distance measure for discrete traits (e.g., Hamming distance), the approach developed here is capable of characterizing such patterns, and determining whether sets of discrete phenotypic differences are enhanced with increasing body size among species. Thus, our approach is the first to our knowledge to facilitate a formal evaluation of both discrete and continuous phenotypic differences between the sexes, providing a comprehensive means of determining whether sets of phenotypic traits differ in a manner as predicted by Rensch's rule.

14

References

Abouheif, E., and D. J. Fairbairn. 1997. A comparative analysis of allometry for sexual size dimorphism: Assessing rensch's rule. The American Naturalist 149:540–562.

Adams, D. C. 1999. Methods for shape analysis of landmark data from articulated structures. Evolutionary Ecology Research 1:959–970.

Adams, D. C., and M. L. Collyer. 2018. Multivariate phylogenetic comparative methods: Evaluations, comparisons, and recommendations. Systematic Biology 67:14–31.

Adams, D. C., and M. L. Collyer. 2019. Phylogenetic comparative methods and the evolution of multivariate phenotypes. Annual Review of Ecology, Evolution, and Systematics 50:405–425.

Adams, D. C., and R. Felice. 2014. Assessing trait covariation and morphological integration on phylogenies using evolutionary covariance matrices. PLoS ONE 9:e94335.

Adams, D. C., and E. Otárola-Castillo. 2013. Geomorph: An r package for the collection and analysis of geometric morphometric shape data. Methods in Ecology and Evolution 4:393–399.

Adams, D. C., F. J. Rohlf, and D. E. Slice. 2013. A field comes of age: Geometric morphometrics in the 21st century. Hystrix 24:7–14.

Adams, D., M. Collyer, and A. Kaliontzopoulou. 2019. Geomorph: Software for geometric morphometric analyses. r package version 3.1.1.

Altman, D. G., and J. M. Bland. 1983. Measurement in medicine: The analysis of method comparison studies. The Statistician 32:307–317.

Andersson, M. 1994. Sexual selection. Princeton University Press.

Astúa, D. 2010. Cranial sexual dimorphism in new world marsupials and a test of renschs rule in didelphidae. Journal of Mammalogy 91:1011–1024.

Berns, C. M., and D. C. Adams. 2013. Becoming different but staying alike: Patterns of sexual size and shape dimorphism in bills of hummingbirds. Evolutionary Biology 40:246–260.

Blanckenhorn, W. U., R. C. Stillwell, K. A. Young, C. W. Fox, and K. G. Ashton. 2006. When rensch meets

bergmann: Does sexual size dimorphism change systematically with latitude? Evolution 60:2004–2011.

Blows, M. W. 2007. A tale of two matrices: Multivariate approaches in evolutionary biology. Journal of Evolutionary Biology 20:1–8.

Bolnick, D. I., and M. Doebeli. 2003. Sexual dimorphism and adaptive speciation: Two sides of the same ecological coin. Evolution 57:2433–2449.

Bonduriansky, R. 2007. Sexual selection and allometry: A critical appraisal of the evidence and ideas. Evolution 61:838–849.

Bookstein, F. L. 1997. Landmark methods for forms without landmarks: Morphometrics of group differences in outline shape. Medical Image Analysis 1:225–243.

Bookstein, F. L. 1991. Morphometric tools for landmark data: Geometry and biology. Cambridge University Press, Cambridge.

Braña, F. 1996. Sexual dimorphism in lacertid lizards: Male head increase vs female abdomen increase? Oikos 75:511–523.

Burbrink, F. T., and I. Futterman. 2019. Female-biased gape and body-size dimorphism in the new world watersnakes (tribe: Thamnophiini) oppose predictions from renschs rule. Ecology and Evolution 9:9624–9633.

Butler, M. A., T. W. Schoener, and J. B. Losos. 2000. The relationship between sexual size dimorphism and habitat use in greater antillean *Anolis* lizards. Evolution 54:259–272.

Ceballos, C. P., D. C. Adams, J. B. Iverson, and N. Valenzuela. 2013. Phylogenetic patterns of sexual size dimorphism in turtles and their implications for Rensch's rule. Evolutionary Biology 40:194–208.

Collyer, M. L., and D. C. Adams. 2018. RRPP: An R package for fitting linear models to high-dimensional data using residual randomization. Methods in Ecology and Evolution 9:1772–1779.

Collyer, M. L., D. J. Sekora, and D. C. Adams. 2015. A method for analysis of phenotypic change for phenotypes described by high-dimensional data. Heredity 115:357–365.

Cox, R. M., S. L. Skelly, and H. B. John-Alder. 2003. A comparative test of adaptive hypotheses for sexual size dimorphism in lizards. Evolution 57:1653–1669.

Dale, J., P. O. Dunn, J. Figuerola, T. Lislevand, T. Székely, and L. A. Whittingham. 2007. Sexual selection

16

explains renschs rule of allometry for sexual size dimorphism. Proceedings of the Royal Society B: Biological Sciences 274:2971–2979.

Darwin, C. R. 1871. The descent of man, and selection in relation to sex. J. Murray, London.

Dayan, T., and D. Simberloff. 2005. Ecological and community-wide character displacement: The next generation. Ecology Letters 8:875–894.

Emlen, D. J. 2008. The evolution of animal weapons. Annual Review of Ecology, Evolution, and Systematics 39:387–413.

Endler, J. A. 1983. Natural and sexual selection on color patterns in poeciliid fishes. Environmental Biology of Fishes 9:173–190.

Fairbairn, D. J. 1997. Allometry for sexual size dimorphism:Pattern and process in the coevolution of body size in males and females. Annual Review of Ecology and Systematics 28:659–687.

Fairbairn, D. J. 2013. Odd couples - extraordinary differences between the sexes in the animal kingdom. Princeton University Press.

Fairbairn, D. J., and R. F. Preziosi. 1994. Sexual selection and the evolution of allometry for sexual size dimorphism in the water strider, Aquarius remigis. American Naturalist 144:101–118.

Fairbairn, D. J., W. U. Blanckenhorn, and T. Székely. 2007. Sex, size and gender roles. Oxford University Press.

Garcia-Navas, V., T. Bonnet, R. Bonal, and E. Postma. 2015. The role of fecundity and sexual selection in the evolution of size and sexual size dimorphism in new world and old world voles (rodentia: Arvicolinae). Oikos 125:1250–1260.

Geist, V., and M. Bayer. 1988. Sexual dimorphism in the cervidae and its relation to habitat. Journal of Zoology 214:45–53.

Gunz, P., P. Mitteroecker, S. Neubauer, G. W. Weber, and F. L. Bookstein. 2009. Principles for the virtual reconstruction of hominin crania. Journal of Human Evolution 57:48–62.

Haas, G. 1973. Muscles of the jaws and associated structures in the rhynchocephalia and squamata. Pp. 285–490 *in* C. Biology of the reptilia vol. 4. Gans and T. Parsons, eds. Academica Press.

Herrel, A., R. V. Damme, and F. D. Vree. 1996. Sexual dimorphism of head size in podarcis hispanica

atrata: Testing the dietary divergence hypothesis by bite force analysis. Netherlands Journal of Zoology 46:253–262.

Hirst, A. G., and T. Kiørboe. 2014. Macroevolutionary patterns of sexual size dimorphism in copepods. Proceedings of the Royal Society B: Biological Sciences 281:20140739.

Holliday, C. M., and N. M. Gardner. 2012. A new eusuchian crocodyliform with novel cranial integument and its significance for the origin and evolution of crocodylia. PLoS ONE 7:e30471.

Horne, C. R., A. G. Hirst, and D. Atkinson. 2020. Selection for increased male size predicts variation in sexual size dimorphism among fish species. Proceedings of the Royal Society B: Biological Sciences 287:20192640.

Huyghe, K., B. V. Hooydonck, H. Scheers, M. Molina-Borij, and R. V. Damme. 2005. Morphology, performance and fighting capacity in male lizards, *Gallotia galloti*. Functional Ecology 19:800–807.

Johnson, P. J., M. J. Noonan, A. C. Kitchener, L. A. Harrington, C. Newman, and D. W. Macdonald. 2017. Rensching cats and dogs: Feeding ecology and fecundity trends explain variation in the allometry of sexual size dimorphism. Royal Society Open Science 4:170453.

Kaliontzopoulou, A., D. C. Adams, A. van der Meijden, A. Perera, and M. A. Carretero. 2012. Relationships between head morphology, bite performance and ecology in two species of podarcis wall lizards. Evolutionary Ecology 26:825–845.

Kaliontzopoulou, A., M. A. Carretero, and D. C. Adams. 2015. Ecomorphological variation in male and female wall lizards and the macroevolution of sexual dimorphism in relation to habitat use. Journal of Evolutionary Biology 28:80–94.

Kaliontzopoulou, A., M. A. Carretero, and G. A. Llorente. 2010. Intraspecific ecomorphological variation: Linear and geometric morphometrics reveal habitat-related patterns within *podarcis bocagei* wall lizards. Journal of Evolutionary Biology 23:1234–1244.

Kelly, C. D., K. E. Folinsbee, D. C. Adams, and M. D. Jennions. 2013. Intraspecific sexual size and shape dimorphism in an australian freshwater fish differs with respect to a biogeographic barrier and latitude. Evolutionary Biology 40:408–419.

Lailvaux, S. P., and D. J. Irschick. 2007. The evolution of performance-based male fighting ability in

caribbean anolis lizards. The American Naturalist 170:573–586.

Lande, R. 1979. Quantitative genetic analysis of multivariate evolution, applied to brain: Body size allometry. Evolution 33:402–416.

Lande, R., and S. J. Arnold. 1983. The measurement of selection on correlated characters. Evolution 37:1210–1226.

Littleford-Colquhoun, B. L., C. Clemente, G. Thompson, R. H. Cristescu, N. Peterson, K. Strickland, D. Stuart-Fox, and C. H. Frere. 2019. How sexual and natural selection shape sexual size dimorphism: Evidence from multiple evolutionary scales. Functional Ecology 33:1446–1458.

Lovich, J. E., and J. W. Gibbons. 1992. A review of techniques for quantifying sexual size dimorphism. Growth, Development, and Aging 56:269–281.

Meiri, S., A. E. Kadison, M. Novosolov, P. Pafilis, J. Foufopoulos, Y. Itescu, P. Raia, and D. Pincheira-Donoso. 2014. The number of competitor species is unlinked to sexual dimorphism. Journal of Animal Ecology 83:1302–1312.

Mitteroecker, P., and P. Gunz. 2009. Advances in geometric morphometrics. Evolutionary Biology 36:235–247.

O'Keefe, F. R., H. P. Street, B. C. Wilhelm, C. D. Richards, and H. Zhu. 2011. A new skeleton of the cryptoclidid plesiosaurTatenectes laramiensisreveals a novel body shape among plesiosaurs. Journal of Vertebrate Paleontology 31:330–339.

Östman, O., and D. Stuart-Fox. 2011. Sexual selection is positively associated with ecological generalism among agamid lizards. Journal of Evolutionary Biology 24:733–740.

Peñalver-Alcázar, M., P. Galán, and P. Aragón. 2019. Assessing rensch's rule in a newt: Roles of primary productivity and conspecific density in interpopulation variation of sexual size dimorphism. Journal of Biogeography 46:2558–2569.

Peterson, T., and G. B. Müller. 2016. Phenotypic novelty in EvoDevo: The distinction between continuous and discontinuous variation and its importance in evolutionary theory. Evolutionary Biology 43:314–335.

R Core Team. 2019. R: A language and environment for statistical computing. R Foundation for Statistical Computing, Vienna, Austria.

Regis, K. W., and J. M. Meik. 2017. Allometry of sexual size dimorphism in turtles: A comparison of mass

563 and length data. PeerJ 5:e2914.

564 Reiss, M. J. 1986. Sexual dimorphism in body size: Are larger species more dimorphic? Journal of Theoretical
565 Biology 121:163–172.

566 Rensch, B. 1950. Die abhangigkeit der relativen sexualdifferenz von der korpergrosse. Bonner Zoologische
567 Beitraege 1:58–69.

568 Rensch, B. 1960. Evolution above the species level. Columbia University Press.

569 Rohlf, F. J., and M. Corti. 2000. The use of partial least-squares to study covariation in shape. Systematic
570 Biology 49:740–753.

571 Rohlf, F. J., and D. E. Slice. 1990. Extensions of the procrustes method for the optimal superimposition of
572 landmarks. Systematic Zoology 39:40–59.

573 Serrano-Meneses, M.-A., and T. Szekely. 2006. Sexual size dimorphism in seabirds: Sexual selection, fecundity
574 selection and differential niche-utilisation. Oikos 113:385–394.

575 Stamps, J. 1983. Sexual selection, sexual dimorphism and territoriality. Pp. 169–204 *in* Lizard ecology:
576 studies of a model organism. Huey R.B., Pianka E.R., and T. Schoener, eds. Harvard University Press.

577 Stephens, P. R., and J. J. Wiens. 2009. Evolution of sexual size dimorphisms in emydid turtles: Ecological
578 dimorphism, rensch's rule, and sympatric divergence. Evolution 63:910–925.

579 Stuart-Fox, D. 2008. A test of rensch's rule in dwarf chameleons (bradypodion spp.), a group with female-
580 biased sexual size dimorphism. Evolutionary Ecology 23:425–433.

581 Stuart-Fox, D., and A. Moussalli. 2007. Sex-specific ecomorphological variation and the evolution of sexual
582 dimorphism in dwarf chameleons (bradypodion spp.). Journal of Evolutionary Biology 20:1073–1081.

583 Tarr, S., S. Meiri, J. J. Hicks, and A. C. Algar. 2018. A biogeographic reversal in sexual size dimorphism
584 along a continental temperature gradient. Ecography 42:706–716.

585 Wagner, G. P., and L. Altenberg. 1996. Perspective: Complex adaptations and the evolution of evolvability.
586 Evolution 50:967.

587 Wagner, G. P., and G. B. Muller. 2002. Evolutionary innovations overcome ancestral constraints: A re-
588 examination of character evolution in male sepsid flies (diptera: Sepsidae). Evolution and Development

20

4:1–6.

Watson, N. L., and L. W. Simmons. 2010. Mate choice in the dung beetle onthophagus sagittarius: Are female horns ornaments? Behavioral Ecology 21:424–430.

Figure Legends

Figure 1. (A) Sexual size dimorphism for males and females across 100 hypothetical species. The pattern displayed exhibits a slope > 1.0, and thus corresponds to Rensch's rule. (B) The same data represented as the ratio of M/F sizes plotted against average species size. (C) Sexual dimorphism represented as the distance between males and females: $SDD = D_{M:F}$. (D) Sexual dimorphism represented as an index of the SD Distance: $SDDI = \pm 1 * D_{M:F}$. In all panels, the dashed line corresponds to values representing no sexual dimorphism (the 1:1 line).

Figure 2. Results of phylogenetic simulations testing the type I error and statistical power for detecting patterns consistent with Rensch's rule. Vertical bars represent the proportion of datasets found to be significant. For type I error analyses, the dashed line marks the standard threshold of $\alpha = 0.05$. For univariate data, both phylogenetic regression of male versus female size (standard approach), and $SDDI$ versus overall body size (new approach) were performed. For multivariate data, only $SDDI$ versus overall body size was examined.

Figure 3. (A) Set of linear measurements used to obtain head proportions. HL: head length, HW: head width, HH: head height, PL: pileus length, MO: mouth opening. (B) Locations of 17 landmarks (1-10; 17) and semilandmarks (11-16) used to quantify head shape. (C) Patterns of sexual size dimorphism represented as male versus female size. (D) Patterns of sexual size dimorphism, represented as sexual size dimorphism index ($SSDI$) versus mean size. (E) Multivariate patterns sexual dimorphism in body proportions ($SShDI$) versus mean size. (F) Multivariate patterns of sexual shape dimorphism ($SShDI$) versus mean size. In panels C, D, E, and F, the red line indicates the regression estimate obtained from the data, while the dashed line corresponds to values representing no sexual dimorphism.

Figure 4. Principal components plot of male (black squares) and female (red points) species mean head shape: the first two PC axes explain over 60% of the total shape variation. Green lines correspond to the sexual shape dimorphism in one of the smallest species, *Lacerta agilis bosnica*, and in the largest species, *Timon lepidus*. Thin-plate spline deformation grids display the mean head shape for males and females of these species.

A Size Dimorphism

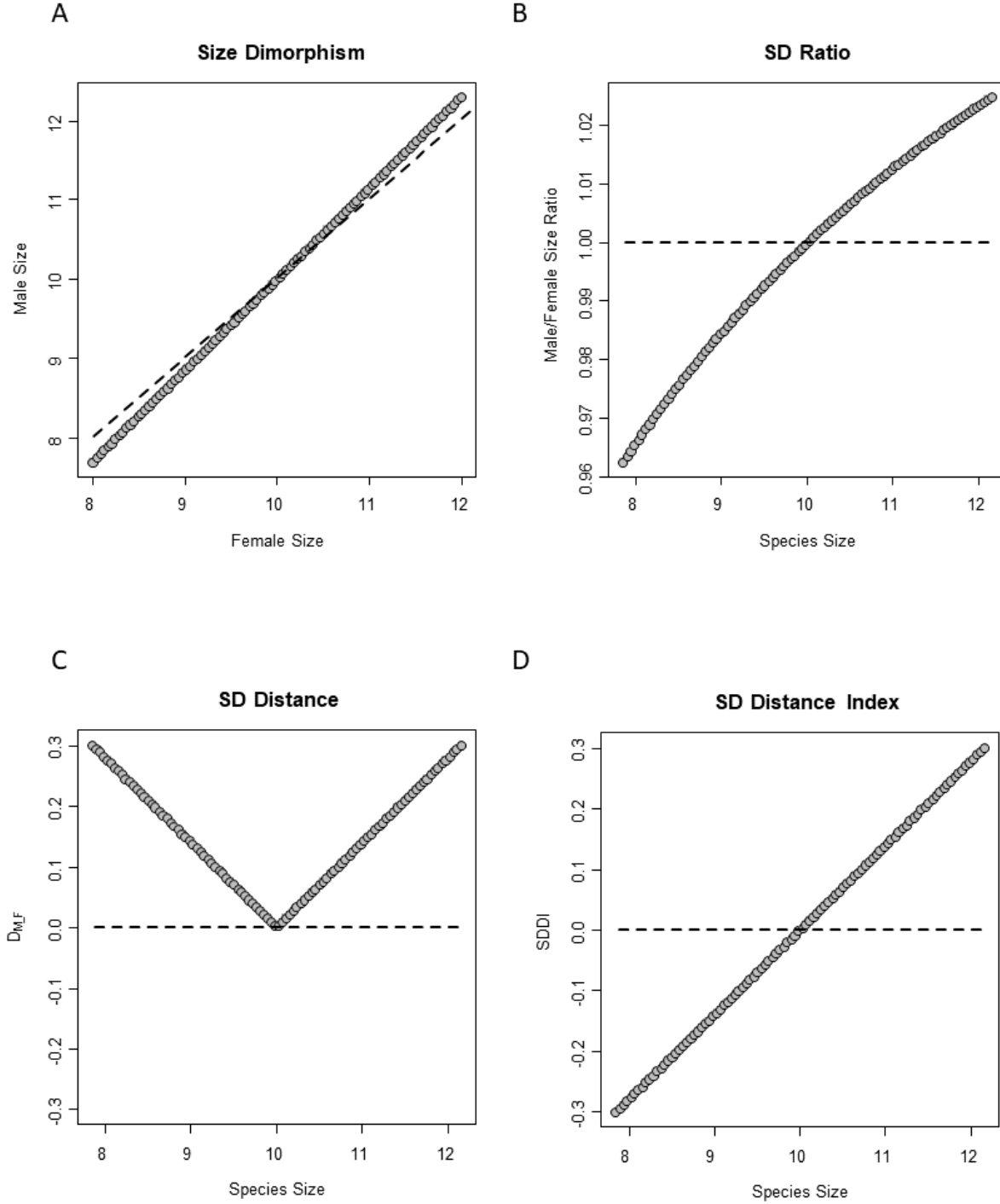**B** SD Ratio

C SD Distance

D SD Distance Index

Figure 1. (A) Sexual size dimorphism for males and females across 100 hypothetical species. The pattern displayed exhibits a slope > 1.0, and thus corresponds to Rensch's rule. (B) The same data represented as the ratio of M/F sizes plotted against average species size. (C) Sexual dimorphism represented as the distance between males and females: $SDD = D_{M:F}$. (D) Sexual dimorphism represented as an index of the SD Distance: $SDDI = \pm 1 * D_{M:F}$. In all panels, the dashed line corresponds to values representing no sexual dimorphism (the 1:1 line).
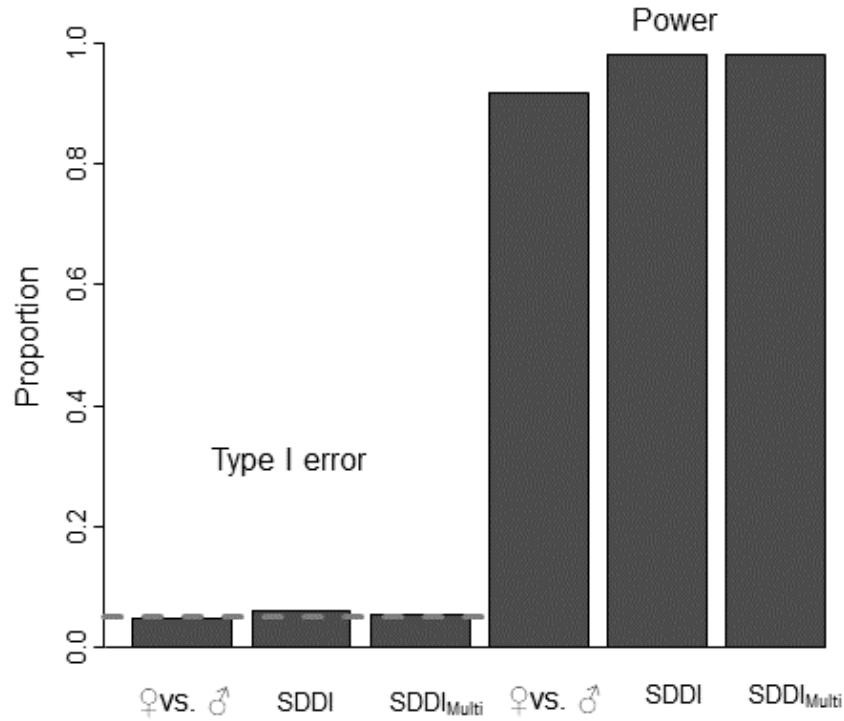
Figure 2. Results of phylogenetic simulations testing the type I error and statistical power for detecting patterns consistent with Rensch's rule. Vertical bars represent the proportion of datasets found to be significant. For type I error analyses, the dashed line marks the standard threshold of $\alpha = 0.05$. For univariate data, both phylogenetic regression of male versus female size (standard approach), and $SDDI$ versus overall body size (new approach) were performed. For multivariate data, only $SDDI$ versus overall body size was examined.
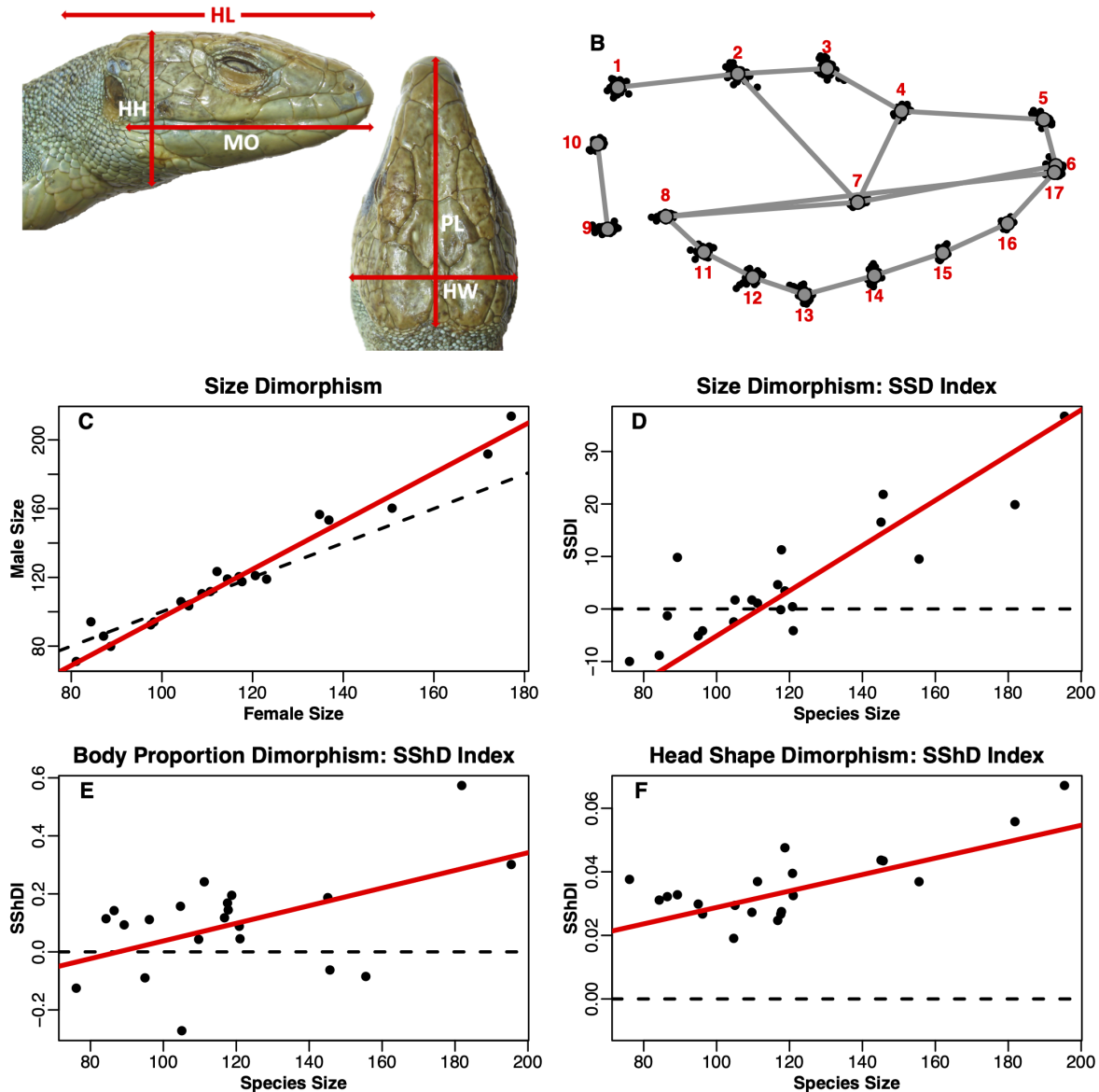
Figure 3. (A) Set of linear measurements used to obtain head proportions. HL: head length, HW: head width, HH: head height, PL: pileus length, MO: mouth opening. (B) Locations of 17 landmarks (1-10; 17) and semilandmarks (11-16) used to quantify head shape. (C) Patterns of sexual size dimorphism represented as male versus female size. (D) Patterns of sexual size dimorphism, represented as sexual size dimorphism index ($SSDI$) versus mean size. (E) Multivariate patterns sexual dimorphism in body proportions ($SShDI$) versus mean size. (F) Multivariate patterns of sexual shape dimorphism ($SShDI$) versus mean size. In panels C, D, E, and F, the red line indicates the regression estimate obtained from the data, while the dashed line corresponds to values representing no sexual dimorphism.
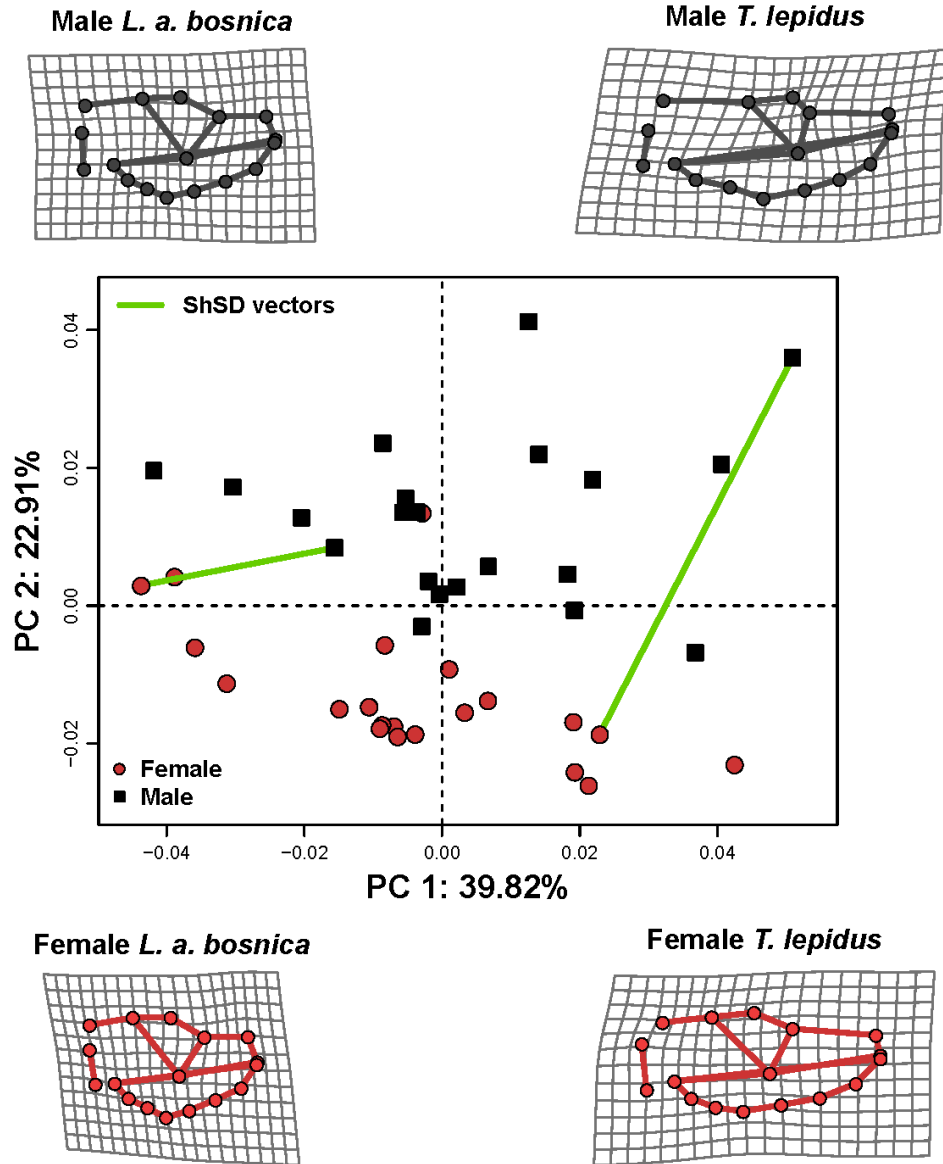
Figure 4. Principal components plot of male (black squares) and female (red points) species mean head shape: the first two PC axes explain over 60% of the total shape variation. Green lines correspond to the sexual shape dimorphism in one of the smallest species, *Lacerta agilis bosnica*, and in the largest species, *Timon lepidus*. Thin-plate spline deformation grids display the mean head shape for males and females of these species.
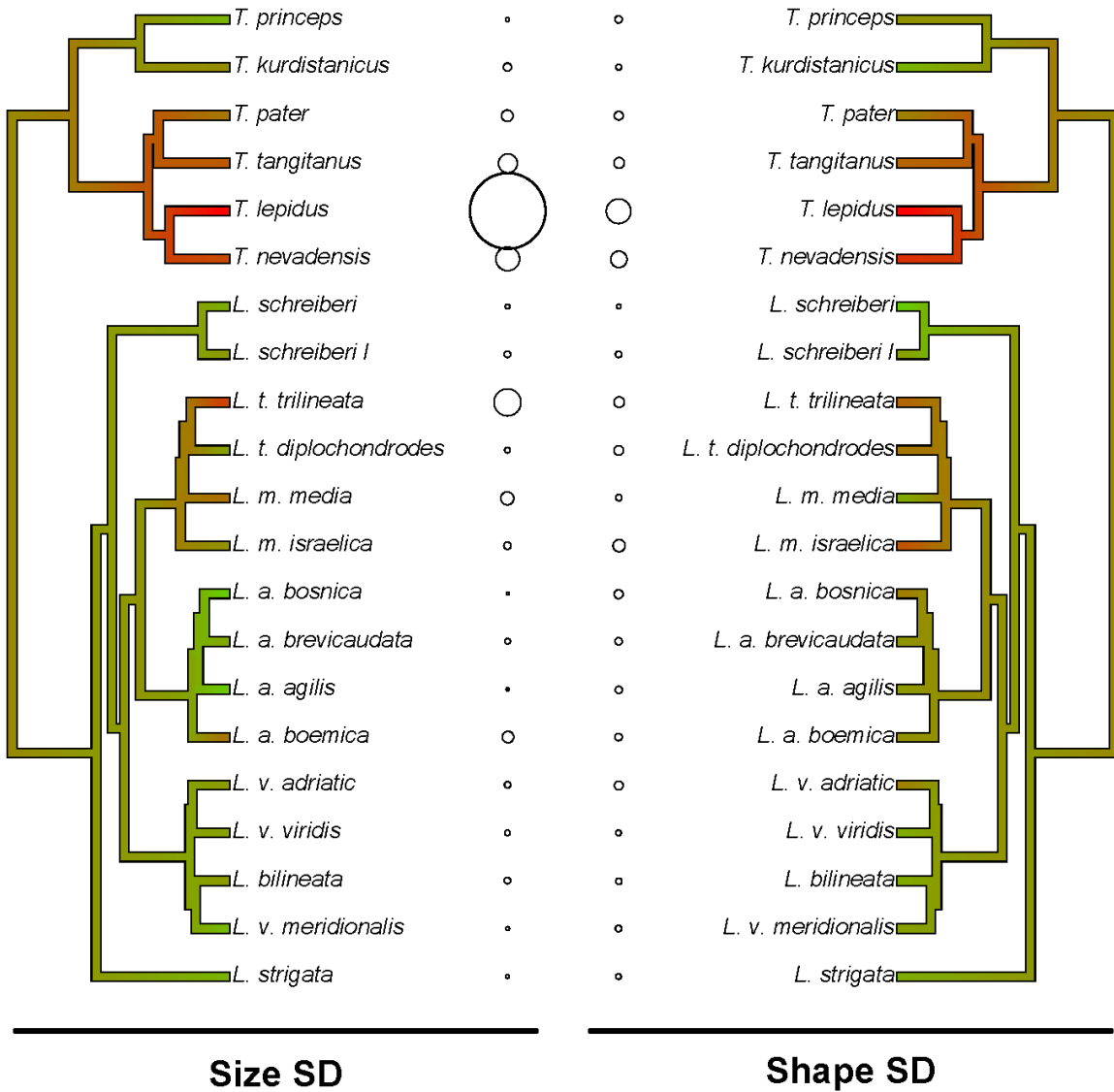
Size SD

Shape SD

660

Figure 5. Heat maps (green: lower values; red: higher values) displaying the evolution of (A) sexual size dimorphism, and (B) sexual shape dimorphism across the phylogeny. For each panel, an index of sexual size dimorphism ($SSDI$) or sexual shape dimorphism ($SShDI$) is displayed, with circles being proportional to the degree of sexual dimorphism.

665